CYBERNETICS AND PHYSICS, VOL. 14, NO. 4, 2025, 334–341

TOWARDS CALIBRATION OF CIRCULAR ULTRASOUND TRANCEIVER ARRAYS

Oleg Granichin
St. Petersburg State University
St. Petersburg, Russia
o.granichin@spbu.ru

Pavel Shcherbakov
Institute of Control Sciences, RAS
Moscow, Russia &
Moscow Institute of Physics and Technology
Dolgoprudny, Russia
cavour118@mail.ru

Olga Granichina
Herzen State Pedagogical University
Saint Petersburg, Russia
olga_granichina@mail.ru

Stepan Trofimov
St. Petersburg State University
St. Petersburg, Russia
steve.trofimov@gmail.com

Ming Yuchi
Huazhong University
of Science and Technology
Wuhan, China
m.yuchi@gmail.com

Article history:
Received 30.11.2025, Accepted 20.12.2025

Abstract

We consider a planar circular array of ultrasound emitter-receiver elements. Due to manufacturing reasons, the actual positions of the elements slightly differ from the ideal equidistant positions exactly on the circle; also, there exist delays in emitting and receiving the signals. This leads to corrupted resulting ultrasound images, and these misplacements and delays are to be evaluated in order to obtain better images. It is assumed that the only available information that we possess is the noisy measurements of the times between the instant of activation of every sensor and the instant of registration of the signal at the receiver. Some of the existing approaches to this *calibration problem* have various drawbacks such as very high dimensions of the associated convex optimization problem or convergence to local minima in nonconvex formulations, etc. To solve this problem, we developed a very simple iterative procedure that requires solving moderately-sized systems of linear equations. At every iteration, we first optimize by a part of variables and then use their updated values to optimize over the rest of the variables. With simple tricks, both problems are converted into linear ones, thus making solution very fast. Preliminary experiments over synthetic data testify to a rather promising performance of the method.

Key words

ultrasound tranceivers, planar circular array, manufacturing imperfections, calibration, iterative method, systems of linear equations, randomized algorithm, stochastic optimization

1 Introduction

Female breast cancer has surpassed lung cancer as the leading cause of global cancer incidence in 2020. Traditional handheld ultrasound imaging is one of the major imaging tools for breast cancer screening in Russia and China; however, it suffers a number of drawbacks. It uses reflection signals for imaging, the patient is usually in the supine position during scanning, the linear array probe is close to the breast skin, and about 10 ml of liquid gel coupling agent is used. The probe can be rotated and translated, the breast tissue can be examined from multiple perspectives. In such a scenario, examination results are dependent on the technique and experience of the technician.

As a potential competitor imaging method for the early detection of breast cancer, ultrasound computed tomography (USCT) technology has been developed rapidly in recent years. Compared with traditional handheld 2D ultrasound devices that use reflection signals for image reconstruction, the USCT system employs a large number of array elements around the imaging object, where the reflection signals are used for structural (reflection) image reconstruction and the transmission signals are used for tissue parameter (sound speed and attenuation) images reconstruction.

In breast USCT imaging, the patient is in a prone position during scanning, and the breast hangs down in

the scanning chamber. Through pre-designed mechanical movements, multi-layer ultrasound tomographic images or whole breast 3D images are scanned and reconstructed, the dependence on technicians is minimized, and the standardization of acquisition can be realized.

Since relatively recently, USCT is being widely used in medical imaging also due to its non-invasive nature and low cost of the equipment. A number of ultrasound imaging systems have been developed specifically for breast cancer screening, [Durić et al., 2007, Ruiter et al., 2012, Lenox, 2015, Song et al., 2022], and [Zhang et al., 2025]; and algorithms have been proposed to reconstruct the structure of the region under analysis based on the results provided via use of these devices, [Jovanović, 2008, Roy et al., 2011, Wang et al., 2020], and [Fang et al., 2022]. In this paper, we analyze one of the aspects of improving the accuracy of image reconstruction in USCT.

A large group of the USCT methods for recovery of high-resolution images relies on measuring *time of flight* (ToF) of the signal between an emitter and a receiver. The speed of sound depends on the density of media it propagates in, hence, based on these measurements, it is possible to reconstruct the density map of specific 2D sections of the analyzed tissue with the succeeding diagnosis being formulated.

However, these measurements are hard to perform precisely. Indeed, typically, the diameter of the circular array used in medical USCT is 20 to 25cm, and the speed of sound (in water) is approximately $1\,500$m/sec, depending on the temperature [Durić et al., 2007]. That means that the time of flight is at most a fraction of a millisecond, which is quite difficult to measure accurately. Also, the sensors located close to each other have high noise/signal ratio due to even much smaller ToF between them; hence, such measurements are not quite reliable.

Moreover, and most importantly, due to imperfections of the manufacturing process, the actual positions of sensors differ from the ideal ones, which are equidistant on the circle, and the distances between sensors are not known precisely. By the same manufacturing reasons, there exist delays in emitting and receiving the signals, the first one being the time gap between the moment of activation of the transmitting sensor and the actual moment of emission. This equally applies to signal reception delays.

The magnitudes of these imperfections are very small; still, since the speed of sound in different types of tissue varies only slightly, these inaccuracies pose serious difficulties in reconstructing the density map from the final ultrasound image. Therefore, to obtain a clean image, it is crucial to detect these imperfections as precisely as possible. We refer to this detection procedure as *calibration*.

Mathematically, from the optimization point of view, the existing approaches to calibration can be roughly divided into two groups.

The first approach works directly with the Cartesian coordinates of the sensors. Then, shaping a certain performance index as a function of the coordinates and delays with the succeeding minimization, it is possible to recover the misplacements and actual delays. Thus, a global optimization approach to finding the actual locations of sensors was proposed in [Rahaman et al., 2023]. However, the performance functional in [Rahaman et al., 2023] is a nonconvex function; hence, such method sometimes converges to local minima, and multiple restarts from various initial points are required. Also, the algorithm was tested over a 28-sensor array, whereas the approach presented in our paper enables processing much larger arrays. A similar approach proposed in [Lin et al., 2021] suffers the same local-minima drawback.

Within the second approach (e.g., see [Roy et al., 2011] as a typical paper), the problem is reformulated in terms of distances between the elements; it then becomes convex, so that solving it by means of any reasonable optimization procedure leads to the unique, global optimum. However the crucial difficulty in solving this specific problem is a huge number of variables and huge dimensions of the coefficient matrices, which severely complicates data storage and the solution itself. With n being the amount of sensors, these quantities are of the order of $(\frac{n^2-n}{2}+2n+1)$ and $n^2\times(n^2+2n)$, respectively, which is highly laborious to tackle for $n=1\,000$ and higher. Also, recovery of coordinates from distances requires application of the so-called *Miltidimensional Scaling* procedure, which incorporates additional inaccuracies in the computational scheme.

To solve this calibration problem, in this paper we propose a simple iterative method of a totally different flavor. At every iteration it requires one matrix-vector multiplication of size $2n$ and solving n times a system of two linear equations in two variables.

Preliminary versions of this paper are [Granichin et al, 2024] and [Granichin et al., 2025]; here, we present more accurate formulations about the noise in the measurements, change the structure of the method, modify the motivation, logic, and the overall presentation of the material.

2 Assumptions and Formulation of the Problem

Schematically, a typical array of sensors is depicted in Fig. 1. To formulate the problem of our interest, we let n denote the amount of sensors and adopt several assumptions.

The first basic assumption is the availability of noise-corrupted *observations*

$$m_{ij}=t_{ij}+e_i+r_j+\varepsilon_{ij},\quad i,j=1,\dots,n,\quad i\neq j, \tag{1}$$

where $t_{ij}, i,j=1,\dots,n$, is the actual time of flight of the signal between emitter i and receiver j; $e_i, r_i, i=1,\dots,n$, are emission and reception delays; and ε_{ij} is

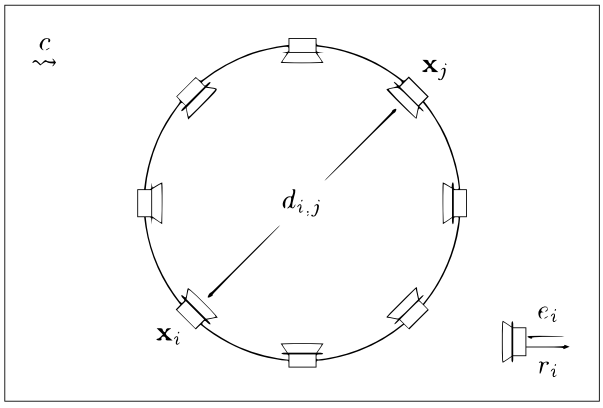

Figure 1. A scheme of a circular array of ultrasound sensors

the observation noise; see below for a detailed description. The quantities t_{ij}, e_i, r_i are not known, and the only information we possess is the set of noisy measurements m_{ij} of the time elapsed from the time instants between the activation of emitter i and the registration of the signal arrived at emitter j. By arrival we understand the registration of the first peak magnitude of the signal by a receiver.

By the very physics of the process, this last instant cannot be measured precisely; in particular, because of the continuous nature of the signal propagation and the digital, quantized nature of the sensors. To reflect this inconsistency, we introduce errors ε_{ij} in the time measurements (1). They are assumed to be independent random variables having identical continuous probability distribution with zero mean and symmetric with respect to the mean. Moreover, the support set of the ε_{ij}s is assumed to be finite and bounded by slightly more than a half of the quantization time of a sensor. The most natural distribution in this class is the uniform one, though truncated Gaussian, triangular, etc. may be considered.

The second assumption is the precise enough knowledge of the speed of signals. It can either be measured directly, or the following formula for the speed of sound in pure water under normal conditions may be used, [Lubbers and Graaff, 1998]:

$$c \approx 1\,404.03 + 4.7\,T - 0.04\,T^2,$$

where T is the temperature (Celsius). Numerous experiments confirmed rather high accuracy of this formula for temperatures between $15^\circ \le T \le 35^\circ$.

As the third assumption, for simplicity we consider the purely planar shape of the array, though the method presented below can be reformulated for three-dimensional coordinates of the sensors.

Finally, we omit the presence of other possible manufacturing inaccuracies, e.g., such as incorrect orientation of sensors leading to non-planar directions of emitted signals, and the like.

Now, denote by $x_i = (x_{i1}, x_{i2})^\top \in \mathbb{R}^2$ the coordinates of sensor i on the plane, and the distance $d_{ij} = \|x_i - x_j\|_2$ between emitter i and receiver j. Then we have

$$(x_{i1} - x_{j1})^2 + (x_{i2} - x_{j2})^2 = (ct_{ij})^2, \qquad i < j. \quad (2)$$

The problem is to evaluate the x_is, e_is, r_is, and t_{ij}s from data (1) and relations (2).

3 The Proposed Iterative Method

At every iteration of the method we separately evaluate the delays and the coordinates (the latter is referred to as *triangulation*) by solving low-dimensional systems of linear equations, so that every step of the method consists of two stages where the optimization is performed over a part of variables. In other words, our algorithm can be considered as a version of the *Block Coordinate Descent*; e.g., see [Bertsekas, 1999].

The initial guess of the iterative procedure is $e_i^0 = r_i^0 = 0$, and x_i^0 are taken to be "ideal" positions of the sensors located precisely equidistantly on the circle. Respectively, at step s we have approximations e_i^s, r_i^s, and x_i^s, $i = 1, \dots, n$.

We now describe how the two stages of iteration $(s+1)$ are executed.

3.1 The first stage: Estimates of the delays are updated

Having x_i^ss, we update $e_i^s \to e_i^{s+1}$ and $r_i^s \to r_i^{s+1}$. To this end, introduce

$$t_{ij}^s = \frac{1}{c}\Big((x_{i1}^s - x_{j1}^s)^2 + (x_{i2}^s - x_{j2}^s)^2\Big)^{1/2}, \quad i < j, \quad (3)$$

according to (2), and first sum up equations (1) over i for every j to obtain the following n linear equations in $2n$ variables e_i, r_i:

$$\sum_{\substack{i=1\\ i\neq j}}^{n} e_i + (n-1) r_j = \sum_{\substack{i=1\\ i\neq j}}^{n} (m_{ij} - t_{ij}^s) + \sum_{\substack{i=1\\ i\neq j}}^{n} \varepsilon_{ij}, \; j = 1, \dots, n. \quad (4)$$

Similarly, we sum up equations (1) over j for every i to obtain yet another set of n linear equations:

$$(n-1) e_i + \sum_{\substack{j=1\\ j\neq i}}^{n} r_j = \sum_{\substack{j=1\\ j\neq i}}^{n} (m_{ij} - t_{ij}^s) + \sum_{\substack{j=1\\ j\neq i}}^{n} \varepsilon_{ij}, \; i = 1, \dots, n. \quad (5)$$

We refer to operations in (4) and (5) as *summation trick*.

We rewrite equations (4)-(5) in the compact form as

$$C \begin{pmatrix} e \\ r \end{pmatrix} = v^s + \varepsilon,$$

where

$$C = \begin{pmatrix} \mathbf{1}_{n\times n} & (n-1) I_{n\times n} \\ (n-1) I_{n\times n} & \mathbf{1}_{n\times n} \end{pmatrix} - I_{2n\times 2n} \in \mathbb{R}^{2n\times 2n} \quad (6)$$

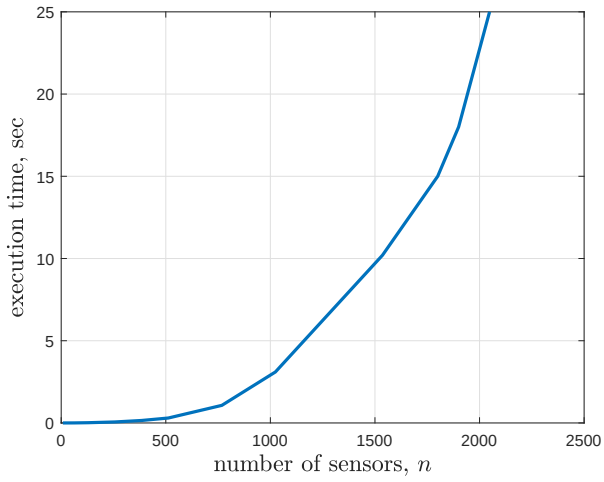

Figure 2. Execution time for the peudoinverse routine `pinv` in MATLAB as function of the matrix size

is the matrix composed of the coefficients at the left-hand sides of equations (4)-(5), whereas $\mathbf{1}_{n\times n} \in \mathbb{R}^{n\times n}$ and $I_{n\times n} \in \mathbb{R}^{n\times n}$ are the all-ones and the identity matrices, respectively; $e = (e_1, \dots, e_n)^\top, r = (r_1, \dots, r_n)^\top$ are the variables; $v^s \in \mathbb{R}^{2n}$ is the vector of the data m_{ij} and estimates t_{ij} on the right-hand sides of equations (4)-(5), and $\varepsilon \in \mathbb{R}^{2n}$ is the cumulative vector of errors ε_{ij} shaped in accordance with (4)–(5).

Now, to find the $(s+1)$st-step approximations to the delays e_i, r_i, we use the standard least squares approach; its correct application is justified by the assumptions on the noise (independence, identical distribution, and unbiasedness).

Two comments regarding the summation above are due at this point.

First, having estimates t_{ij}s, we might consider the initial data representation (1) and apply the least squares procedure. However, the amount of equations in (1) is $(n^2 - n)$, whereas we arrived at a much less sizeable set of $2n$ equations. Second, by summing up, we "improve" the statistical properties of the reidual ε,—due to the adopted properties of the ε_{ij}.

The coefficient matrix C (6) is seen to be singular, with the eigenvector corresponding to the zero eigenvalue having the form

$$p = t/\|t\|; \quad t = (\underbrace{1, \dots, 1}_{n}, \underbrace{-1, \dots, -1}_{n})^\top.$$

The rest of the eigenvalues are $\lambda = 2(n-1)$, $\mu = -n$, and $\nu = n-2$, the latter two having multiplicity $n-1$.

Hence, as the $(s+1)$st-step approximations to the delays e_i, r_i we adopt the least squares solution

$$\begin{pmatrix} e^{s+1} \\ r^{s+1} \end{pmatrix} = C^+ v^s,$$

where C^+ is the Moore–Penrose pseudoinverse of C, see [Albert, 1972].

It is important to note that the matrix C remains unchanged at all iterations, so the pseudoinverse operation is to be performed only once, prior to starting the iterative process. This is a very attractive salient feature of our method, because as the dimensionality of the matrix (i.e., the number of sensors) increases, the computation time grows extremely fast and reaches about 25sec on a "standard" laptop for $n = 2\,048$ (see Fig. 2 for an illustration), which is a "typical" amount for modern ultrasound equipment. This observation shows the benefits of the summation trick. Finally, the matrix-vector multiplication above comes at almost no cost.

3.2 The second stage: Estimates of the positions are updated

At this point we have approximations $x_i^s = (x_{i1}^s,\ x_{i2}^s)^\top \in \mathbb{R}^2$, $i = 1, \dots, n$, to the true positions x_i, and the approximations e_i^{s+1}, r_i^{s+1}, $i = 1, \dots, n$, to the delays.

Having all this data, consider a fixed element i and update its estimate x_i^s. To this end, we treat x_i as a variable, pick an arbitrary (say, randomly chosen) trial pair x_j^s, x_k^s, where $j \neq k \neq i$, and consider $e_i^{s+1}, r_j^{s+1}, r_k^{s+1}$. Since $t_{ij} = m_{ij} - e_i - r_j - \varepsilon_{ij}$ by (1), from (2) we have

$$(x_{i1} - x_{j1}^s)^2 + (x_{i2} - x_{j2}^s)^2 = c^2\,(m_{ij} - e_i^{s+1} - r_j^{s+1} - \varepsilon_{ij})^2 \tag{7}$$

and

$$(x_{i1} - x_{k1}^s)^2 + (x_{i2} - x_{k2}^s)^2 = c^2\,(m_{ik} - e_i^{s+1} - r_k^{s+1} - \varepsilon_{ik})^2. \tag{8}$$

Let us now split the right-hand sides of (7) and (8) into two terms: The first one, call it f_{ij}^{s+1} (respectively, f_{ik}^{s+1}) accumulates all error-free quantities, and the second one, call it δ_{ij}^{s+1} (respectively, δ_{ik}^{s+1}) accumulates all error-dependent quantities. Expanding the brackets on the left-hand sides of these two equations and extracting the second equation from the first one, we arrive at the relation

$$\begin{aligned} 2x_{i1}(x_{k1}^s - x_{j1}^s) + 2x_{i2}(x_{k2}^s - x_{j2}^s) + \|x_j^s\|^2 - \|x_k^s\|^2 \\ = f_{ij}^{s+1} - f_{ik}^{s+1} + \delta_{ij}^{s+1} - \delta_{ik}^{s+1}, \end{aligned}$$

which is linear in x_{i1}, x_{i2}. This operation will be referred to as the *removal-of-squares trick*. With the shorthand notation:

$$a_{jk1}^s x_{i1} + a_{jk2}^s x_{i2} = u_{ij}^{s+1} + \mu_{jk}^{s+1}, \tag{9}$$

where the coefficients are given by

$$a_{jk1}^s = 2(x_{k1}^s - x_{j1}^s); \quad a_{jk2}^s = 2(x_{k2}^s - x_{j2}^s) \tag{10}$$

and

$$u_{jk}^{s+1} = f_{ij}^{s+1} - f_{ik}^{s+1} + \|x_k^s\|^2 - \|x_j^s\|^2, \tag{11}$$

$$\mu_{jk}^{s+1} = \delta_{ij}^{s+1} - \delta_{ik}^{s+1}. \tag{12}$$

Similarly, picking another trial pair x_p^s, x_q^s, where $p \neq q \neq j \neq k \neq i$, we obtain the associated linear equation

$$a_{pq1}^s x_{i1} + a_{pq2}^s x_{i2} = u_{pq}^{s+1} + \mu_{pq}^{s+1}, \qquad (13)$$

where the form of the coefficients $a_{pq1}^s, a_{pq2}^s, u_{pq}^{s+1}, \mu_{pq}^{s+1}$ is clear from the context. In the matrix form equations (9), (13) write

$$\begin{pmatrix} a_{jk1}^s & a_{jk2}^s \\ a_{pq2}^s & a_{pq2}^s \end{pmatrix} \begin{pmatrix} x_{i1} \\ x_{i2} \end{pmatrix} = \begin{pmatrix} u_{jk}^{s+1} \\ u_{pq}^{s+1} \end{pmatrix} + \begin{pmatrix} \mu_{jk}^{s+1} \\ \mu_{pq}^{s+1} \end{pmatrix}. \qquad (14)$$

Noting that the coefficient matrix in the last relation is generically nonsingular, application of Least Squares yields the $(s+1)$st-step approximation x_i^{s+1} to the position x_i:

$$x_i^{s+1} = \begin{pmatrix} a_{jk1}^s & a_{jk2}^s \\ a_{pq2}^s & a_{pq2}^s \end{pmatrix}^{-1} \begin{pmatrix} u_{jk}^{s+1} \\ u_{pq}^{s+1} \end{pmatrix}$$

As one of the possible modifications of the method we might consider use of $\ell > 2$ pairs of triangulation points at this stage to improve the numerical stability of the method. In that case, we obtain $\ell > 2$ equations of the form (13) and use pseudoinverse of the associated $\ell \times 2$ coefficient matrix.

We note that a similar "linearization" approach to location reconstruction was proposed in [Sastry, 2023]; however, it assumed the absence of delays e_i, r_j in the observation setup. Moreover, the source of the measurement errors ε_{ij} was basically limited to the quantization of sensors, and the estimates of these errors were obtained from statistical/physical considerations or using specific instrumental tools.

Now, perform these manipulations with other elements i to obtain $(s+1)$st-step approximations to all $x_i, i = 1, \ldots, n$. Iteration s is complete.

We next proceed to step $(s+2)$, etc. until a certain prespecified accuracy is attained or the maximum number of iterations is exceeded.

Specifically, we measure the progress in the estimation by the relative improvement of the estimates

$$\Psi_s = \frac{1}{n}\left(\sqrt{\sum_{i=1}^n \|x_i^s - x_i^{s-1}\|^2} + \sqrt{\sum_{i=1}^n (e_i^s - e_i^{s-1})^2} + \sqrt{\sum_{i=1}^n (r_i^s - r_i^{s-1})^2} \right) \qquad (15)$$

and stop as soon as it becomes negligibly small.

The algorithmic form of the method is given below.

The Calibration Algorithm

Input: Speed c of sound,
number n of sensors,
measurements m_{ij}, $i, j = 1, \ldots, n$,
initial guess x_i^0, e_i^0, r_i^0, $i = 1, \ldots, n$,
tolerance ν, max number of iterations $s_{\max}$

1. Form the matrix C (6), compute its pseudoinverse C^+; set $s := 0$; $\Psi_{s-1} = 0$, $\Psi_s := 100$[1]
2. **while** $(|\Psi_s - \Psi_{s-1}| > \varepsilon) \wedge (s \leq s_{\max})$ **do**:
3. Compute t_{ij}^s (3), compose v^s from the deterministic terms at the right-hand sides of (4), (5)
4. $\begin{pmatrix} e^{s+1} \\ r^{s+1} \end{pmatrix} := C^+ v^s$
5. **for each** $i \in \{1, \ldots, n\}$ **do**:
6. Pick different $j, k, p, q \neq i$ from $\{1, \ldots, n\}$
7. Compute a_{jk}^s, a_{pq}^s via (10), $u_{jk}^{s+1}, u_{pq}^{s+1}$ via (11) and $\mu_{jk}^{s+1}, \mu_{pq}^{s+1}$ via (12)
8. $x_i^{s+1} := \begin{pmatrix} a_{jk1}^s & a_{jk2}^s \\ a_{pq2}^s & a_{pq2}^s \end{pmatrix}^{-1} \begin{pmatrix} u_{jk}^{s+1} \\ u_{pq}^{s+1} \end{pmatrix}$
9. **end for**
10. $s \to s+1$
11. Compute Ψ_s via (15)
12. **end while**

Output: Estimates x_i^s, e_i^s, r_i^s of the positions and delays

It is expected that just a few iterations are needed to obtain an accurate enough final estimate.

4 Simulation Setup and Preliminary Results

4.1 Design of the test data

We tested the algorithm over several sets of low-dimensional "synthetic" data. Specifically, we located n points equidistantly on the circumference of diameter $d = 22$cm and then corrupted their coordinates by random noise uniformly distributed on $[-0.001d, 0.001d]$ to model inaccuracies in the sensor locations; see Fig. 3 for $n = 32$.

To model the values of the measurements m_{ij}, we invoke the actual positions x_i generated above and calculate the distances d_{ij} between the sensors; since the value of c is assumed to be known, we compute the exact values of ToF as $t_{ij} = d_{ij}/c$, which is at most $1.5 \cdot 10^{-4}$s ($\max d_{ij} = 0.22$m; $c = 1500$m/sec). Then, we model the delays as

$$e_i = 0.01 \frac{1}{n} \sum_{j \neq i} t_{ij},\ r_i = e_i + \xi_i;\ \xi_i = \mathcal{U}[-0.01e_i,\ 0.01e_i],$$

where $\mathcal{U}[a, b]$ denotes the uniform distribution over $[a, b]$. In words, the magnitude of each delay e_i was taken to be at most 1% of the mean ToF of signals emitted form emitter i; same for receiver i, with a small random amount added, just to differ from the e_is. Finally, noting that a typical sampling frequency of ultrasonic sensors is about 25MHz, we model the noise ε_{ij} as a random variable uniformly distributed over $[-0.4 \cdot 10^{-7},\ 0.4 \cdot 10^{-7}]$.

[1] Actually, $\Psi_s \ll 100$ for all s, since the absolute values of the quantities involved are very small.

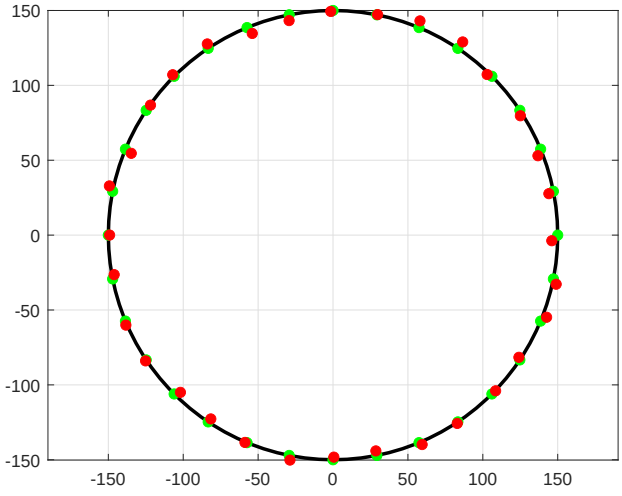

Figure 3. Ideal (green) and actual (red) locations of $n = 32$ sensors, schematically

Overall, the test data (the errors in the ideal locations of sensors, time of flight, and the values of delays) was generated to conform with a typical real-world setup; i.e., both the absolute and relative magnitudes of the quantities involved and small manufacturing imperfections both in the locations and delays seem to be adequate to practice; e.g., see [Roy et al., 2011].

As noted in the introduction, the measurements m_{ij} for sensors i and j located close to each other can have high noise/signal ratio, so the sensors in the trial pairs should be chosen sufficiently distant from the triangulated one. In the experiments, we selected trial pairs randomly uniformly over a subset of sensors that does not include the nearest $n/4$ elements to the left and right of the triangulated sensor.

The performance of the algorithm was measured by

$$\Phi_s = \frac{1}{n}\left(\sqrt{\sum_{i=1}^{n}\|x_i^s - x_i\|^2} + \sqrt{\sum_{i=1}^{n}(e_i^s - e_i)^2} + \sqrt{\sum_{i=1}^{n}(r_i^s - r_i)^2}\right), \tag{16}$$

the cumulative mean square error, where x_i, e_i, r_i are the generated quantities and x_i^s, e_i^s, r_i^s are their sth-step estimates obtained with our method. Note that this performance index differs from the one in (15), since in the "synthetic experiment," the actual positions and delays are known (being generated by us), and such an index is more reliable and easier to interpret.

4.2 Results of simulations and discussion

For each of the various values of $n = 16, 32, 64, 128, \ldots$, we ran our algorithm over $N = 100$ different sets of synthetic data $\{x_i, e_i, r_i, m_{ij},\ i, j = 1, \ldots, n\}$ designed as above, and using the described policy of picking the trial pairs.

The typical performance of the method for $n = 64$ is depicted in Fig. 4. The method is seen to converge very quickly, leading to $\Phi_{12} \approx 10^{-4}$, i.e., after just 12 iterations, the initial error was reduced by a factor of 300; for $s = 16$ iterations, we obtained $\Phi_{16} \approx 10^{-6}$ and $\Phi_{20} \approx 10^{-8}$. A similar or better behavior was observed

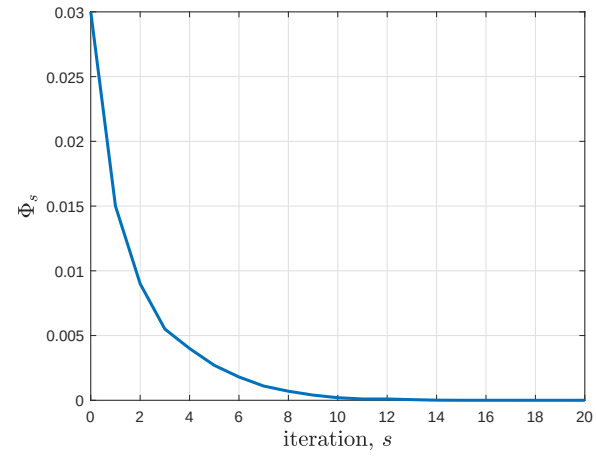

Figure 4. Performance of the algorithm for $n = 64$

for smaller number of sensors, $n = 16$ and $n = 32$.

However, for $n = 128$, after 15 iterations, the process often ($\approx$15% of runs) saturated at $\Phi_{\lim} \approx 10^{-5}$ and there was no further decrease in the performance index. Still, in this case, the accuracy was improved by a factor of 200 to 300. The value of the saturation level and the percentage of "poor" outcomes grow as n increases; moreover, for $n = 2\,048$, the method exposed divergence in 10% of the runs.

A possible explanation for these phenomena could be the accumulation of errors when repeatedly solving sets of linear equations and use of the pseudoinverse of a high-dimensional matrix computed via the floating-point operations. Also, the instability of the algorithm for higher values of n may be explained by the insufficiency of use of just two pairs of trial points for triangulation. These issues are the subject of further refinement of the method.

5 Conclusions and Future Research

We proposed a formulation of a new iterative method for calibration of planar circular arrays of ultrasound sensors; i.e., a method that recovers imprecise locations of the sensors and emitter/receiver delays from the available measurements. The computational complexity of the method is very low, since it requires solving

moderately-sized systems of linear equations. Preliminary numerical experiments over low-dimensional "synthetic" data demonstrated reasonable performance of the method. Needless to say, there is a lot of issues to be addressed in the future research, and below we mention some of the most important ones.

- Note that estimation of the locations of two different sensors is performed independently of each other, so that parallel or distributed computations might be applied to essentially reduce the runtime of the algorithm.
- The procedure needs to be tested over high-dimensional ($n = 2\,048$) real, not synthetic data.
- A theoretical proof of convergence is highly desired.
- To further stabilize the numerical performance of the method, artificial disturbances can be incorporated into the measurements with subsequent use of the so-called *Simultaneous Perturbation Stochastic Approximation* approach, [Spall, 2003]. The associated algorithm can be based on the ideas proposed in [Granichin et al., 2021] and [Erofeeva et al., 2025]. Also, accelerated versions of the method can be implemented along the lines formulated in [Chernov et al., 2025].

6 Acknowledgment

The research presented in Section 3.1 was carried out by O. Granichin, supported by Saint Petersburg University, project no. 121061000159-6. Research of P. Shcherbakov reported in Sections 3.2 and 4.1 was performed under the financial support of the Russian Science Foundation (project No. 21-71-30005-П), https://rscf.ru/en/project/21-71-30005/. Research of O. Granichina in Section 4.2 was carried out with the support of the A.I. Herzen Russian State Pedagogical University (project No. 49VG "Quality of life of Russian teachers: methodology, theory, measurement methods"). Research of M. Yuchi in Sections 1 and 2 was carried out under financial support of the National Key Researchand Development Program of China under Grant 2023YFC2410800,

References

Albert, A. (1972). *Regression and the Moore-Penrose Pseudoinverse*, Boston University Press, Boston, MA.

Bertsekas, D. P. (1999). *Nonlinear Programming*, Athena Scientific.

Chernov A., Erofeeva V., Granichin O., Sudomir A. (2025). Accelerated SPSA-based consensus algorithm for mutual device positioning. In *Proc. 64th IEEE Conf. Decision Control*, Rio de Janeiro, Brazil, Dec. 10–12.

Durić, N., Littrup, P., Poulo, L., et al. (2007). Detection of breast cancer with ultrasound tomography: First results with the Computed Ultrasound Risk Evaluation (CURE) prototype. *Med. Phys.*, **34**(2), pp. 773—785.

Erofeeva, V., Granichin, O., and Tarasova, E. (2025). Zero-order distributed non-stationary optimization for Hölder-smooth problems with unknown-but-bounded noise. *IEEE Access*, **13**, pp. 209658–209679.

Fang, X., Zhou, R., Gan, H., Ding, M., and Yuchi, M. (2022). Time-of-flight completion in ultrasound computed tomography based on the singular value threshold algorithm. *Math. Biosci. Eng.*, **19**(10), pp. 10160–10175.

Granichin O., Erofeeva, V., Ivanskiy, Y., and Jiang, Y. (2021). Simultaneous perturbation stochastic approximation-based consensus for tracking under unknown-but-bounded disturbances. *IEEE Trans. Autom. Control*, **66**(8), pp. 3710–3717.

Granichin, O.N., Granichina, O.A. Trofimov, S.A., and Shcherbakov, P.S. (2024). Calibration of large arrays of ultrasound sensors. *Control of Large Scale Systems*, **112**, pp. 294–309 (in Russian).

Granichin, O., Shcherbakov, P., and Trofimov, S. (2025). Fast calibration of arrays of ultrasonic sensors: A formulation of a novel iterative method. *Proc. 7th Int. Conf. Control Systems, Math. Modeling, Automation and Energy Efficiency* (SUMMA2025), Nov 12–14, 2025, Lipetsk, Russia, paper 80.

Jovanović, I. (2008). *Inverse Problems in Acoustic Tomography: Theory and Applications*. Ph.D. thesis, Swiss Federal Institute of Technology in Lausanne, DOI:10.5075/epfl-thesis-4165.

Lenox, M.W., Wiskin, J., Lewis, M., Darrouzet, S., et al. (2015). Imaging performance of quantitative transmission ultrasound. *Int. J. Biomed. Imaging*, Oct., 28, DOI: 10.1155/2015/454028.

Lin, L., Hu, P., Tong, X., et al. (2021). High-speed three-dimensional photoacoustic computed tomography for preclinical research and clinical translation. *Nature Communications*, **12**, article no. 882.

Lubbers, J. and Graaff, R. (1998). A simple and accurate formula for the sound velocity in water. *Ultrasound in Medicine and Biology*, **24**(7), pp. 1065–1068.

Rahaman, J., Prakash, R., Ranjbaran M., et al. (2023) Transducer misplacement compensation for in-lab-made 3D photoacoustic tomography systems using nature-inspired algorithms. In: *Photons Plus Ultrasound: Imaging and Sensing*, **12379**, article no. 123790W. DOI: 10.1117/12.2651216

Roy, O., Jovanović, I., Durić, N., Poulo, N., and Vetterli, M. (2011). Robust array calibration using time delays with application to ultrasound tomography. In *Medical Imaging 2011: Ultrasonic Imaging, Tomography, and Therapy*, **7968**, pp. 46–56 (*Proc. SPIE, The International Society for Optical Engineering*).

Ruiter, N.V., Zapf, M., Hopp. T., et al. (2012). 3D ultrasound computer tomography of the breast: A new era? *European J. Radiol.*, 2012, **81**, suppl. 1: S133–S134, DOI: 10.1016/S0720-048X(12)70055-4.

Sastry, K., Zhang, Y., Hu, P., et al. (2023). A method for the geometric calibration of ultrasound transducer

arrays with arbitrary geometries. *Photoacoustics*, **32**, p. 100520.

Song, J., Zhang, Q., Zhou, L., et al. (2022). Design and implementation of a modular and scalable research platform for ultrasound computed tomography. *IEEE Trans. Ultrasonics, Ferroelectrics, and Frequency Control*, 2022, **69**(1), pp. 62–72.

Spall, J. C. (2003). *Introduction to Stochastic Search and Optimization: Estimation, Simulation, and Control*. Wiley–Interscience, New York.

Wang, S., Zeng, L., Song, J., Zhou, L., Ding, M., Yuchi, M. (2020). Variational mode decomposition for ultrasound computed tomography. In:*Proc. Medical Imaging 2020: Ultrasonic Imaging and Tomography*, **11319**, DOI: 10.1117/12.2549161.

Zhang, Q., Guo, X., Zhang, L., et al. (2025). Real-time reflection imaging system for ultrasound computed tomography with a circular ring array. *IEEE Sensors Journal*, **25**(15), pp. 29830–29840.